

Figure 1: Plot of a Gaussian centered at the middle of an array and the shifted Gaussian by half the array length. The shift is implemented using FFT.

- 1) To shift the function $f(x)$ by amount y , we notice

$$(f * \delta_y)(x) = \int_{-\infty}^{\infty} f(u) \delta(x - y - u) du = \int_{-\infty}^{\infty} f(u) \delta(u - x + y) du = f(x - y)$$

for $\delta_y(x) = \delta(x - y)$, i.e. we need to convolve the input array with a delta function. This is implemented in `assignment6.py`. The plot of a shifted Gaussian is shown in Figure 1.

- 2) a) The correlation function of two arrays is implemented in `assignment6.py`. The correlation function of a Gaussian with itself is shown in Figure 2.
- b) The plot of the correlation function of a Gaussian with the same Gaussian by shifted by different amount is shown in Figure 3. From Figure 3, we can see that the greater the shift, the closer the correlation function peak to the original Gaussian. The height of the correlation function does not depend on the shift.
- 3) The safe convolution algorithm is implemented in `assignment6.py`. The input arrays with length m, n are each padded with zeros at the end to a total length of $m + n - 1$.

- 4) a) We have

$$\sum_{x=0}^{N-1} \exp\left(-\frac{2\pi i k x}{N}\right) = \sum_{x=0}^{N-1} \left[\exp\left(-\frac{2\pi i k}{N}\right) \right]^x = \frac{1 - \exp(-2\pi i k)}{1 - \exp(-\frac{2\pi i k}{N})}$$

which is a summation of a geometric series

$$\sum_{x=0}^{N-1} \alpha^x = \sum_{x=1}^N \alpha^{x-1} = \frac{1 - \alpha^N}{1 - \alpha}.$$

- b) For $k \rightarrow 0$, we have

$$\lim_{k \rightarrow 0} \frac{1 - \exp(-2\pi i k)}{1 - \exp(-\frac{2\pi i k}{N})} = \lim_{k \rightarrow 0} \frac{2\pi i \exp(-2\pi i k)}{\frac{2\pi i}{N} \exp(-\frac{2\pi i k}{N})} = N.$$

For $k \in \mathbb{Z} \neq nN, n \in \mathbb{Z}$, we have

$$\frac{1 - \exp(-2\pi i k)}{1 - \exp(-\frac{2\pi i k}{N})} = \frac{1 - 1}{1 - \exp(-\frac{2\pi i k}{N})} = 0$$

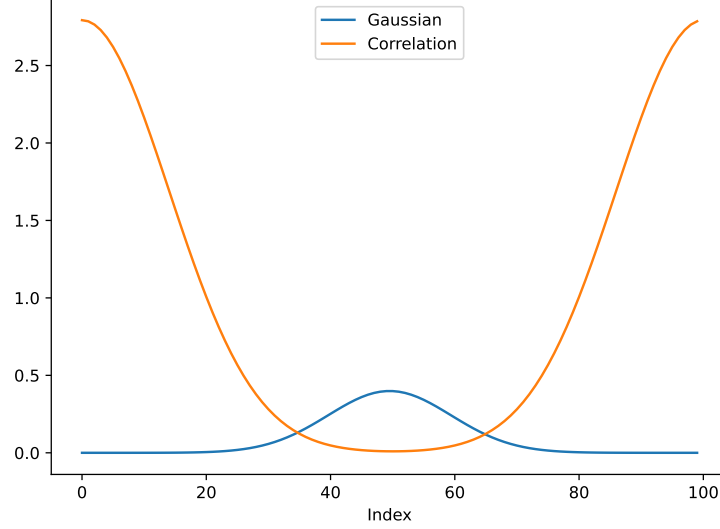


Figure 2: Plot of a Gaussian centered at the middle of an array and its correlation function with itself.

where we note that the denominator is non-zero.

c) We have the analytic DFT of sine function

$$f(x) = \sin \frac{2\pi kx}{N} = \frac{\exp\left(\frac{2\pi i kx}{N}\right) - \exp\left(-\frac{2\pi i kx}{N}\right)}{2i}$$

as

$$\begin{aligned} F(k') &= \sum_{x=0}^{N-1} f(x) \exp\left(-\frac{2\pi i k' x}{N}\right) \\ &= \sum_{x=0}^{N-1} \frac{\exp\left(\frac{2\pi i kx}{N}\right) - \exp\left(-\frac{2\pi i kx}{N}\right)}{2i} \exp\left(-\frac{2\pi i k' x}{N}\right) \\ &= \frac{1}{2i} \left[\sum_{x=0}^{N-1} \exp\left(-\frac{2\pi i (k' - k)x}{N}\right) - \sum_{x=0}^{N-1} \exp\left(-\frac{2\pi i (k' + k)x}{N}\right) \right] \\ &= \frac{1}{2i} \left[\frac{1 - \exp(-2\pi i (k' - k))}{1 - \exp\left(-\frac{2\pi i (k' - k)}{N}\right)} - \frac{1 - \exp(-2\pi i (k' + k))}{1 - \exp\left(-\frac{2\pi i (k' + k)}{N}\right)} \right]. \end{aligned}$$

The plot of NumPy's FFT and the analytic DFT for sine function of $k = 100e$, $N = 1000$ and the residues is shown in Figure 4. Since sine is real, we consider only real FFT. We get

Maximum residue is 4.507629354226542e-11

Average residue is 1.1172617061896613e-12

The residues are of order 10^{-11} at peaks of intensity of order 10^2 . The residues at places of near zero intensity is of order 10^{-12} . This (10^{-12} to 10^{-13} precision) is close to the float precision of 10^{-15} .

d) The FFT of sine function of $k = 100e$, $N = 1000$ multiplies the given window function is shown in Figure 5. From the figure, we can see that the peaks are very narrow and looks like a delta function, which indicates there is little spectral leakage, especially compared with the un-windowed FFT.

e) Numerically, we find

First 5 terms of FFT of the windows function is

[5.00000000e+02+0.00000000e+00j -2.50000000e+02+2.67008637e-14j

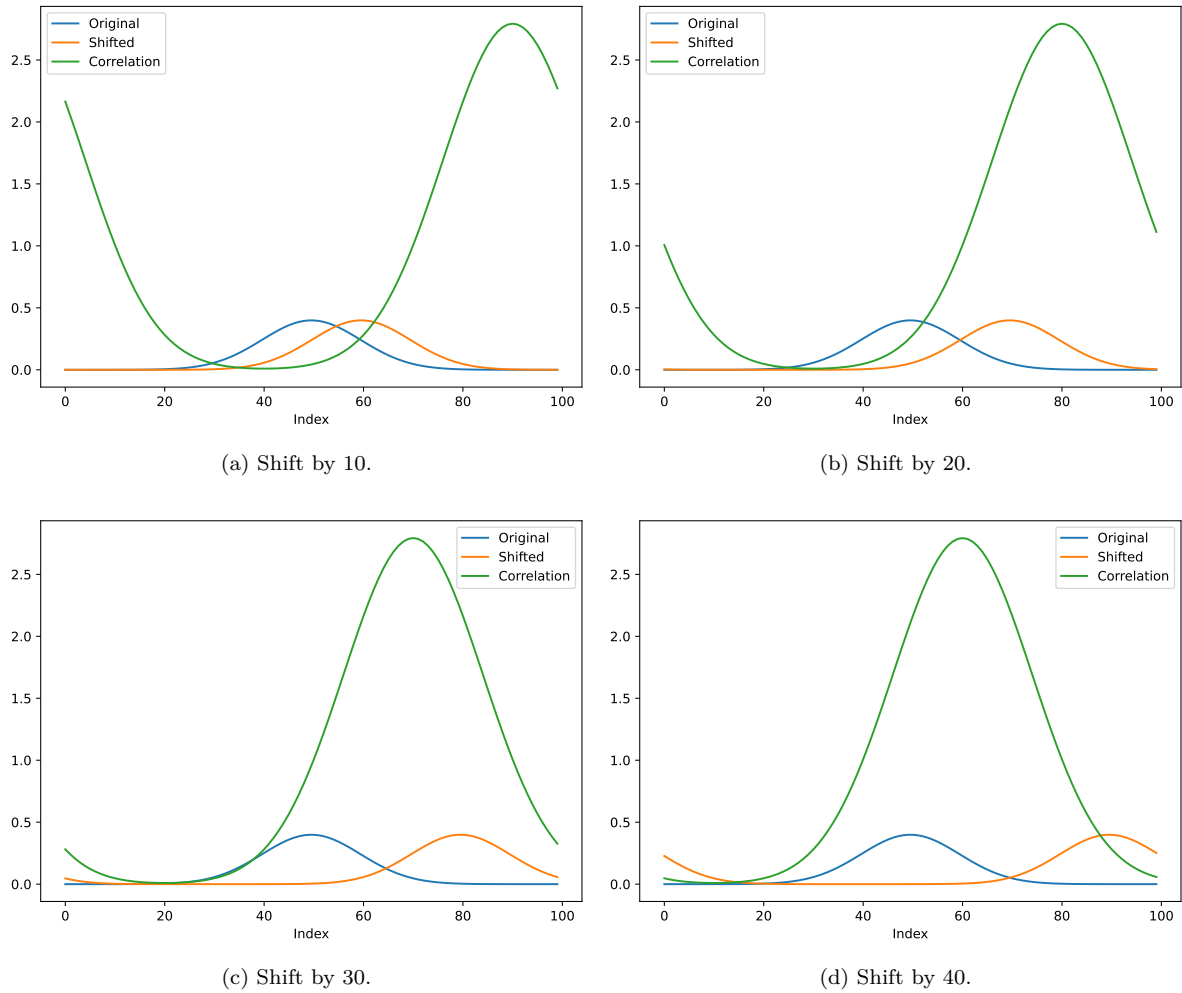


Figure 3: Plot of a Gaussian centered at the middle of an array and its correlation function with itself but shifted by different amount.

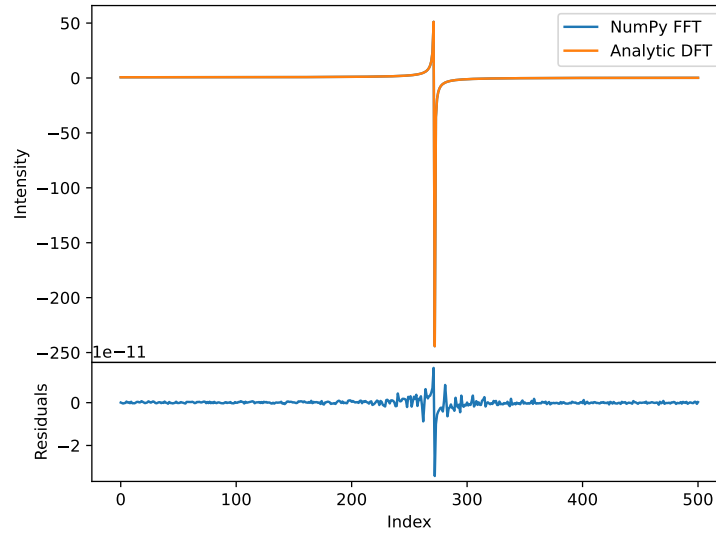


Figure 4: Upper panel shows the plot of NumPy's FFT and the analytic DFT for sine function of $k = e$, $N = 100$. Lower panel shows the residues.

```
-7.39316236e-15+5.53246115e-16j -1.39384937e-15-1.86317880e-15j
 1.64793057e-15+1.61823247e-15j]
```

Last 5 terms of FFT of the windows function is

```
[ 3.22614606e-15-5.81360394e-17j  1.64793057e-15-1.61823247e-15j
 1.41788661e-15+2.36605142e-15j -7.39316236e-15-5.53246115e-16j
-2.50000000e+02-3.37354224e-14j]
```

We can see that the first term is $500 = N/2$, the second term is $-250 = -N/4$ and the last term is $-250 = -N/2$ while other terms are zero (plus some float precision errors), i.e. the FFT of the window function is $N/2, -N/4, 0, \dots, 0, -N/4$.

- 5) a) For the noise model, we first find the Fourier transform of the strain, and the (un-smoothed) noise is estimated to be its absolutely value squared. We use a Planck-Taper window function for the strain before applying FFT, which according to Wikipedia is “first suggested in the context of gravitational-wave astronomy”. It has a flat top which preserves the signal. The noise is then smoothed using `smooth_vector` with a kernel size of 10. This gives us the smoothed noise model as shown in Figure 6. Most of the noise are smoothed, but we still preserves the peaks. Note that we set the smoothed noise with $\nu < 20$ Hz or $\nu > 1500$ Hz as infinite. At $\nu < 20$ Hz, the data from LIGO is not properly calibrated. For $\nu > 1500$ Hz, the data is limited by the sample rate of LIGO.
- b) The noise model is used together with a match filter to find the event. The detected event is shown in Figure 7.
- c) The noise for each event is estimated as mean of the strain and noise's cross correlation's absolute value. The signal is estimated by the difference between the maximum to the minimum. We obtain the noise and SNR estimate as

```
GW150914 at H detection gives noise 0.08895059095890635 and SNR 24.84081816526431
GW150914 at L detection gives noise 0.07831696385762864 and SNR 18.507799791139657
GW150914 detection gives combined SNR 30.977490218360728
LVT151012 at H detection gives noise 0.0588472732843089 and SNR 8.418176526172852
LVT151012 at L detection gives noise 0.05464154988073354 and SNR 7.0979700719426075
LVT151012 detection gives combined SNR 11.011215880546551
GW151226 at H detection gives noise 0.040614550821737 and SNR 13.491308732154922
```

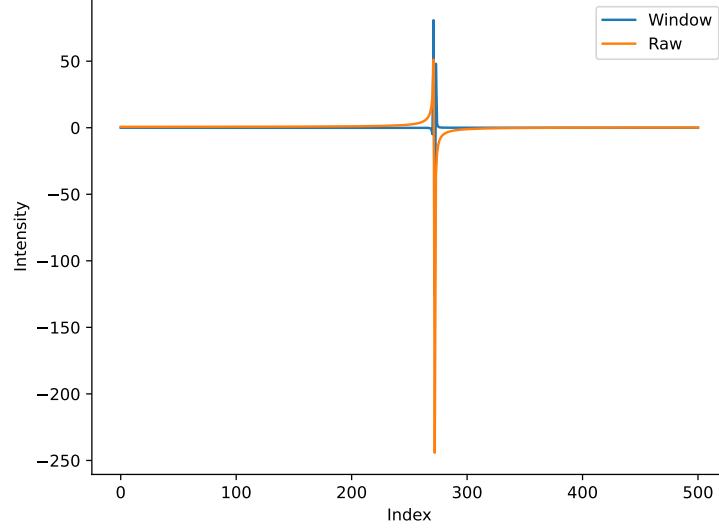


Figure 5: Plot of NumPy's FFT for sine function of $k = e$, $N = 100$ with the given window function.

- GW151226 at L detection gives noise 0.029414990221747265 and SNR 9.91979564196866
 GW151226 detection gives combined SNR 16.745678752583906
 GW170104 at H detection gives noise 0.0735992202293092 and SNR 10.950259528577948
 GW170104 at L detection gives noise 0.09507991718201725 and SNR 13.493697909671099
 GW170104 detection gives combined SNR 17.377803860691785
- d) The analytic value of the noise and SNR is estimated, where use the fact that the analytic noise can be estimated by $\sqrt{A^T N^{-1} A}$. This gives
- GW150914 at H noise model gives noise 1.249422391567653 and SNR 1.7685015656959688
 GW150914 at L noise model gives noise 0.9716631493659766 and SNR 1.491746072980861
 GW150914 noise model gives combined SNR 2.3136343994077615
 LVT151012 at H noise model gives noise 0.9369699688143452 and SNR 0.5287114326813667
 LVT151012 at L noise model gives noise 0.7122205497197538 and SNR 0.5445561573456644
 LVT151012 noise model gives combined SNR 0.7589974885011539
 GW151226 at H noise model gives noise 0.6488006525814316 and SNR 0.8445482321475891
 GW151226 at L noise model gives noise 0.3437533938296436 and SNR 0.8488372683669972
 GW151226 noise model gives combined SNR 1.1974082113433013
 GW170104 at H noise model gives noise 1.0388779736596077 and SNR 0.7757701896141714
 GW170104 at L noise model gives noise 1.302134918541184 and SNR 0.9852893593914549
 GW170104 noise model gives combined SNR 1.254039277225411

The analytic SNR of all four events is much lower than the one given by the match filter.

- e) We obtain the power spectrum using $\mathcal{F}(\text{template})^2/N$ and the frequency for the event is determined. We get

GW150914 at H have frequency (Hz) 117.25962625925361
 GW150914 at L have frequency (Hz) 125.63266133480654
 LVT151012 at H have frequency (Hz) 102.28288137057172
 LVT151012 at L have frequency (Hz) 116.05417303724558
 GW151226 at H have frequency (Hz) 106.35087052113931
 GW151226 at L have frequency (Hz) 143.3825327300126
 GW170104 at H have frequency (Hz) 117.41971852798552
 GW170104 at L have frequency (Hz) 97.32824432323515

- f) For the LIGO detector, the uncertainty in time measurement is $\delta t = 2.44 \times 10^{-4}$ s. As shown in

Figure 8, by simple trigonometry, we have

$$\theta \approx \frac{c\Delta t}{HL}.$$

The uncertainty in θ is approximately proportional to the uncertainty in Δt , so the relative uncertainty in θ is

$$\frac{\delta\theta}{\theta} = \frac{\delta t}{\Delta t}$$

and the absolute uncertainty is

$$\delta\theta = \frac{c\delta t}{L}$$

where we take $c = 3 \times 10^8 \text{ ms}^{-1}$ and $L = 1000 \text{ km}$. We computed the arrival time difference for all four events, and computed this relative and absolute uncertainty

```

GW150914 detection index difference is 30
GW150914 relative uncertainty in angle localization is 0.03333333333333333
GW150914 absolute uncertainty in angle localization is (rad) 0.0732421875
LVT151012 detection index difference is 2
LVT151012 relative uncertainty in angle localization is 0.5
LVT151012 absolute uncertainty in angle localization is (rad) 0.0732421875
GW151226 detection index difference is 5
GW151226 relative uncertainty in angle localization is 0.2
GW151226 absolute uncertainty in angle localization is (rad) 0.0732421875
GW170104 detection index difference is 13
GW170104 relative uncertainty in angle localization is 0.07692307692307693
GW170104 absolute uncertainty in angle localization is (rad) 0.0732421875

```

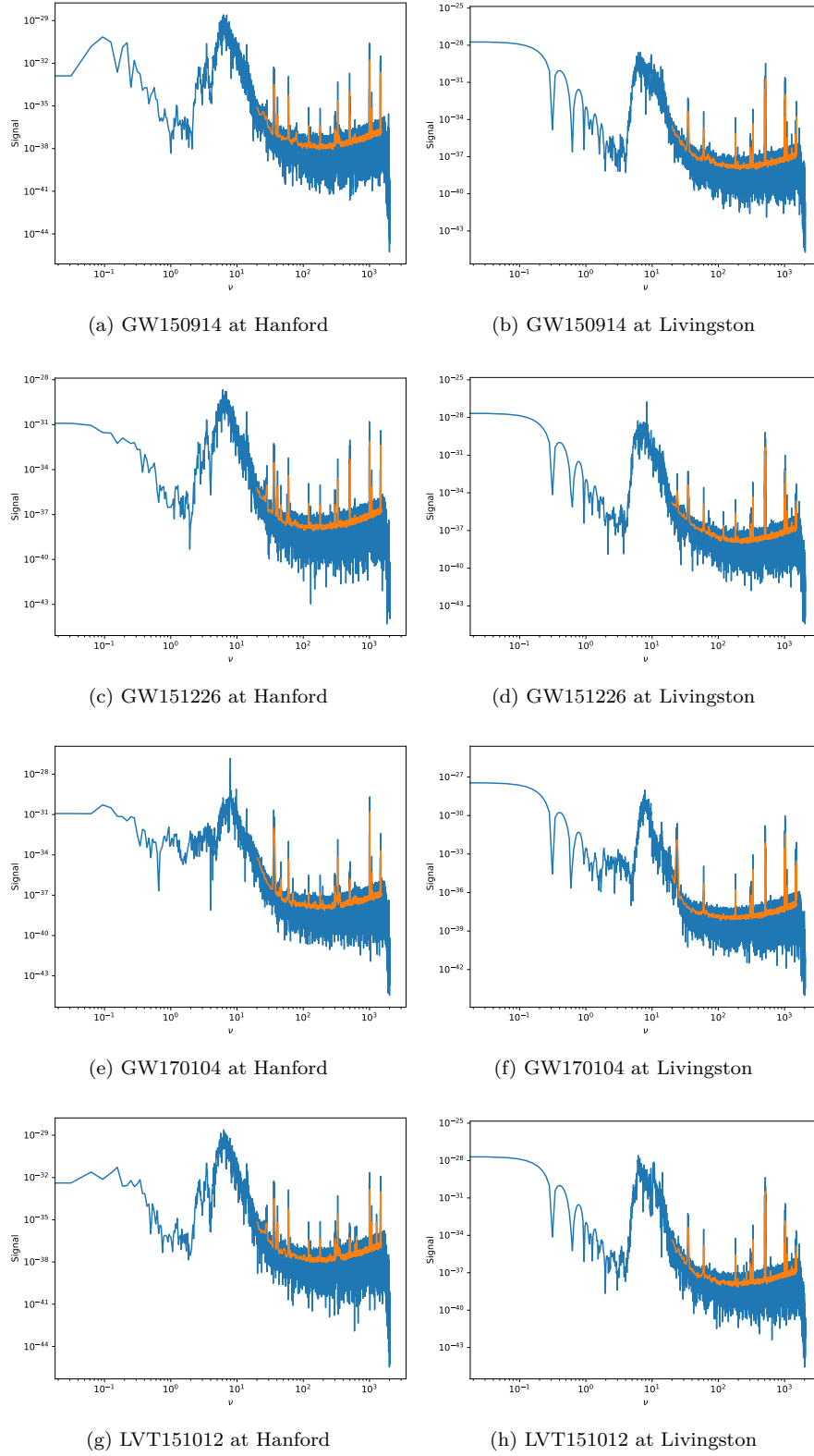
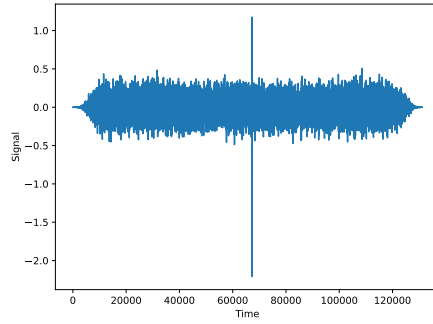
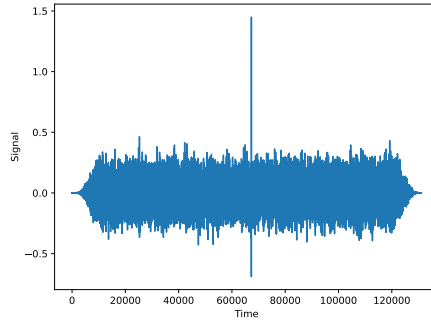


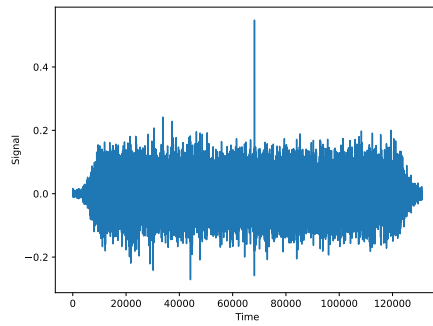
Figure 6: Plot of the smoothed (orange) and un-smoothed (blue) noise model for the four GW events at each detector.



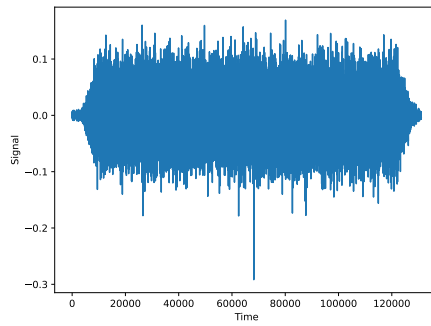
(a) GW150914 at Hanford



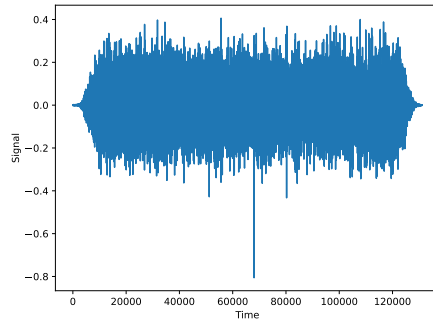
(b) GW150914 at Livingston



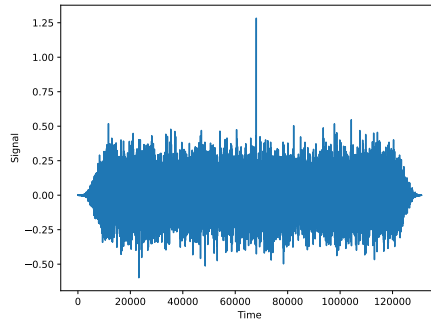
(c) GW151226 at Hanford



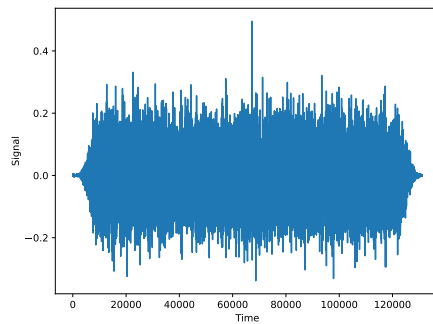
(d) GW151226 at Livingston



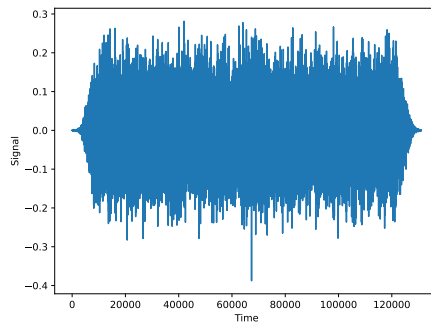
(e) GW170104 at Hanford



(f) GW170104 at Livingston



(g) LVT151012 at Hanford



(h) LVT151012 at Livingston

Figure 7: Event detected for the four GW events at each detector.

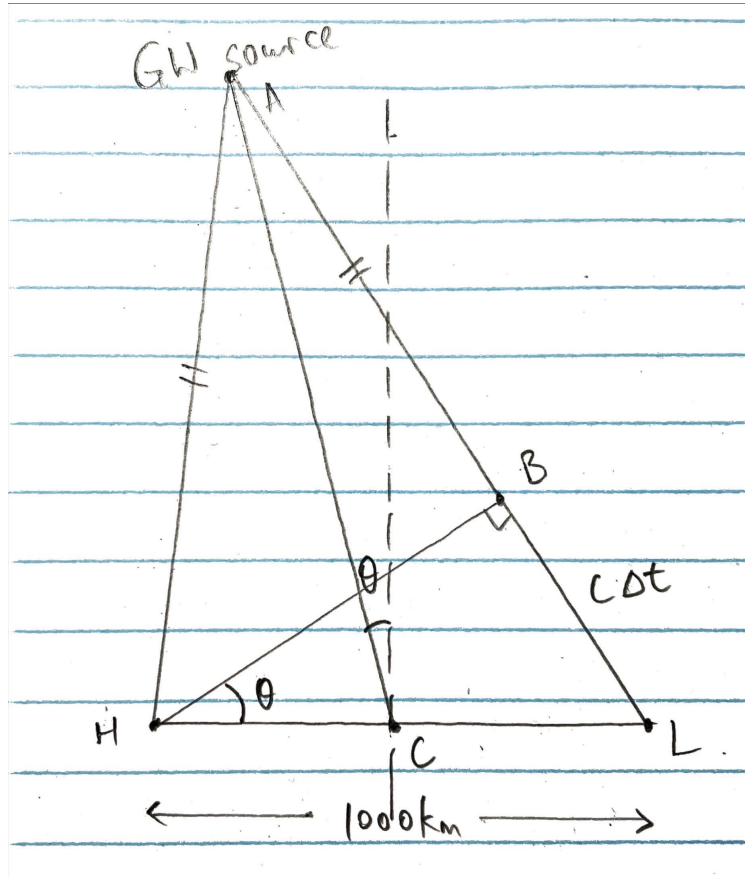


Figure 8: Illustration of the GW detection. This is extremely not to scale. In reality HL is much shorter compared to the distance of AC . This means we can approximate $AH = AB$ and the detection has a time difference of Δt . This is similar to a double slit interference.